Light sources

Light-emitting diodes are simpler to construct, while heterojunction lasers produce lower dispersion and couple to fibers more efficiently; both types have now been operating for well over one year.

Henry Kressel, Ivan Ladany, Michael Ettenberg and Harry Lockwood

The selection of a system for optical communications is largely governed by the availability of the necessary components. Although through-the-atmosphere systems have some applicability, they are generally restricted to small installations where their inherent limitations are tolerable. The optical transmission medium of greater importance for the future is a glass or plastic fiber, and therefore the properties of these fibers—their absorption, dispersion, mechanical strength, and so on—are all-important.

The other determining factor is the requirement that the sources, fibers and detectors used in the system be compatible with one another. Fortunately this compatibility exists-and it is for this reason that optical communications is such a rapidly expanding field. It is generally true that commercially available optical fibers have moderate loss and small dispersion (both modal and material) in the wavelength range 0.8-1.1 microns. In this article we will therefore discuss the current status of semiconductor light sources spanning this wavelength region, and because there are applications for both coherent and incoherent sources we will treat both lasers and LED's (light-emitting diodes).

We will limit our discussion in this article to discrete components. Semiconductor laser components can be expected in the future to move into the area of integrated functions, along the lines described by Esther Conwell in her article on page 48 of this issue of PHYSICS TODAY.

Heterojunction structures

It is only since the advent of the first practical aluminum gallium arsenide-gallium arsenide heterojunction laser structures¹⁻⁵ that the potential of laser diodes for optical communications and other applications has been realized. The GaAs homojunction lasers available earlier had such high threshold and operating

currents as to make them impractical for room-temperature operation. In some heterojunction devices we will describe, threshold current densities have been reduced two orders of magnitude to 500 A/cm² from the homojunction values of about 50 000 A/cm². This progress has made practical a compact continuous-wave laser with high radiance and power output in the range of 10 mW, which can be directly modulated to hundreds of MHz. Figure 1 vividly illustrates the small size and brightness of a cw laser similar in construction to those used in optical communications.

Since optical fibers with losses under 20 dB/km are now commercially available, multi-kilometer, high-data-rate transmission systems (even without repeaters) are expected to become competitive with the existing coaxial systems of electrical communication.

There are also many applications for fiber-optic links over short distances as well as at low data rates (for example, in local distribution systems). The lightemitting diode satisfies many of the requirements of such systems, and because it is not a threshold device its output power is less sensitive than the laser to small changes in operating current or ambient temperature. Much of the technology of LED's is comparable to that of lasers, so that the two devices have tended to be developed together. In fact, state-of-the-art LED's deliver several milliwatts of output power at modulation rates of 100-200 megahertz.

The most highly engineered and tested lasers and LED's for optical communications are those derived from the ternary alloy system Al_xGa_{1-x}As. Thin layers (0.05-1 micron) are sequentially grown with a high degree of perfection by liquid-phase epitaxy on substrates of GaAs. By varying the alloy composition of the recombination region of the direct-band-gap material, 6 the emission wavelength can be varied over a useful range of

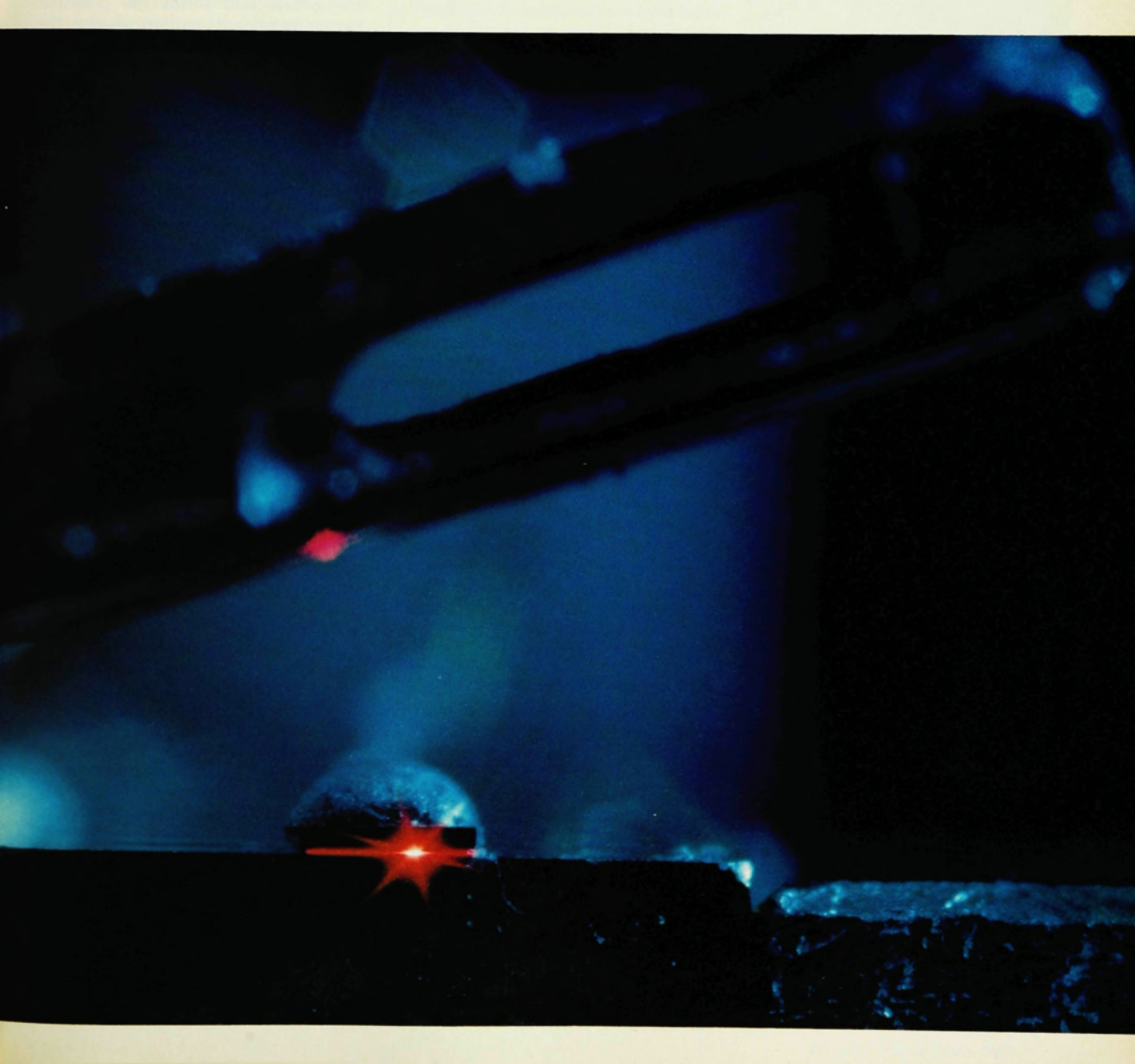
0.8–0.9 microns. Emission, and indeed lasing, can be achieved at still shorter wavelengths but attenuation and dispersion in the fiber begin to become appreciable at shorter wavelengths. The purest (OH-free) fibers available have attenuation and dispersion that decrease to negligible values in the wavelength region of 1.0–1.1 microns, so that there is a real interest in developing new alloy systems and a heterojunction technology for emission in this range also.

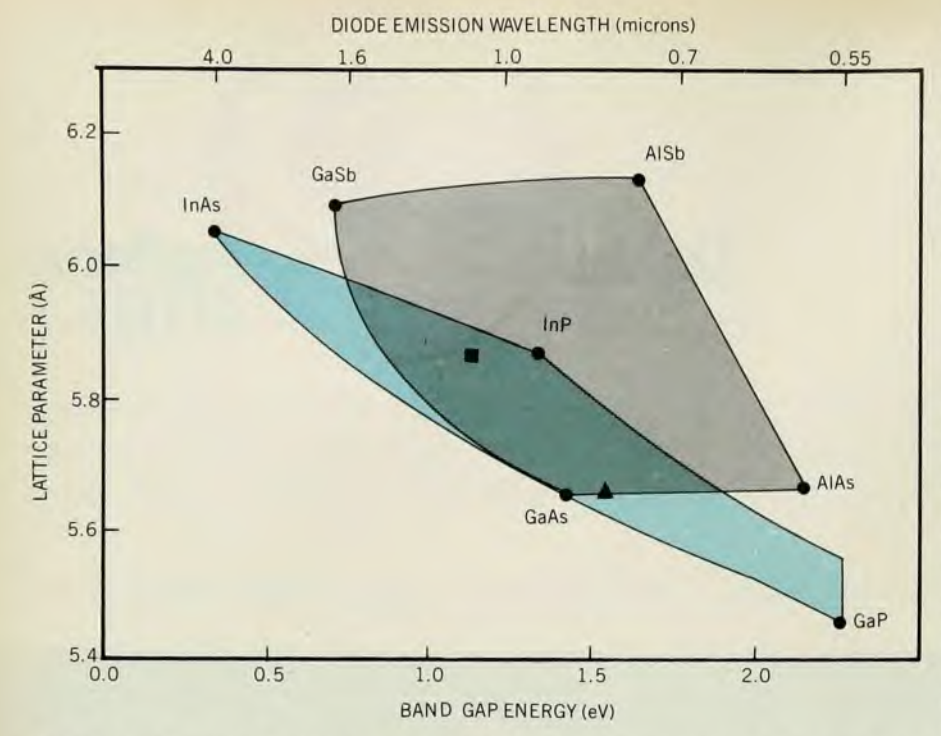
In the Al_xGa_{1-x}As system the lattice parameter varies by only 0.14% as x goes from zero to unity. Heterojunctions in this system consequently have negligible strain-induced defects and demonstrate long-term reliability. In most other ternary alloys, the band gap and lattice parameter vary significantly between the extremes of the binary alloys from which they are derived; Inx Ga1-x As, Inx Ga1-x P and GaAs, P1-x are examples of such alloys. As a result heterojunction structures in these materials contain many defects due to the inevitable strain at the heterojunction interfaces. However, lattice-matching heterojunction structures of indium gallium arsenide-indium gallium phosphide, for example, can be defect free.

An alternative approach to obtaining efficient device performance at 1.0-1.1 microns is to fabricate heterojunction structures in quaternary alloys such as $In_xGa_{1-x}As_yP_{1-y}$ and $Ga_xAl_{1-x}As_y$

Like a Lilliputian beacon, this doubleheterojunction cw laser is dwarfed by an ordinary sewing needle. The aluminum gallium arsenide source shown here, emitting at about 7500 Å, is similar in construction to devices for optical communications, which are designed to emit at about 8200 Å (a wavelength that records poorly on color film). The emitting region of this laser is about 15 microns wide by about 0.5 micron thick. (Photograph courtesy of RCA Labor atories.) Figure 1







Extent of band gaps and lattice parameters covered by the quaternary alloys $Al_xGa_{1-x}As_ySb_{1-y}$ (gray area) and $ln_xGa_{1-x}As_yP_{1-y}$ (colored area). The boundaries of the areas represent ternary, and the vertices binary, alloys. Two particularly useful alloys are indicated: The square (\blacksquare) locates $ln_{0.80}Ga_{0.20}As_{0.35}P_{0.65}$, the lattice parameter of which matches InP substrates and would make diodes that emit at 1.1 microns; the triangle (\blacktriangle) shows the position of $Al_{0.1}Ga_{0.9}As$, which matches the GaAs lattice and emits at about 0.82 microns.

Sb_{1-y}. In these alloys, which cover the desired emission range, the band gap and lattice parameter can be adjusted independently, as figure 2 shows. At some cost in simplicity, this extra degree of freedom permits the fabrication of strain-free heterojunction devices.

As evidenced by a growing literature on the subject, progress towards useful lasers and LED's at about 1.1 microns is being made. Much work, however, remains to ensure their reliability, which is handicapped by lattice defects. Whether the complexity of fabrication will be justified by the moderate improvements in attenuation and dispersion will ultimately be determined by cost and long-term reliability.

The problem of lattice-parameter match at heterojunctions can be discussed in terms of mismatch-dislocation networks. For example, for a 1% lattice mismatch at an interface, a dislocation will be generated at approximately every 100 atom planes. Since the dislocation core consists of nonradiative recombination centers, such a high dislocation density will depress the internal quantum efficiency of the device. Furthermore, dislocations are not always confined to the mismatched interface but can propagate

Henry Kressel is the Head of Semiconductor Device Research, and Ivan Ladany, Michael Ettenberg and Harry Lockwood are members of the technical staff, at the David Sarnoff Research Center of RCA Laboratories. through multilayer structures.

The effect of dislocations on radiative efficiency is dramatically illustrated in figure 3, where we compare a transmission electron photomicrograph of a dislocation array in a mismatched heterojunction structure7 with a cathodoluminescence scan of a similar structure. The dark lines and spots in the cathodoluminescence micrograph are areas of low radiative efficiency, which correspond to dislocations lying parallel and perpendicular to the plane of the surface viewed. Therefore, in designing heterojunction structures for LED's and lasers, it is of extreme importance either to choose a totally lattice-matched system or else to remove dislocations from the active region by compositional grading.

Continuous-operation lasers

Although there are numerous potential configurations for cw laser diodes, the symmetric double heterojunction with a stripe contact has been widely adopted as the simplest laser geometry and that most suitable for optical communications. The schematic and actual cross section of a typical laser, figure 4, shows the optical cavity (recombination region) defined by its higher-band-gap dielectric walls as well as the outer n and p type GaAs regions to which ohmic contact is made.

The efficient operation of a laser diode requires effective minority-carrier and radiation confinement to the optical cavity, which is also the recombination region of the device. Both functions are provided by heterojunctions. Radiation confinement is provided by the dielectric discontinuity, while carrier confinement results from a potential barrier created by the difference in band gap between the materials that form the heterojunction. The average carrier-pair density injected into the recombination region of a double-heterojunction device for a current density J is

$$\Delta N \approx J\tau/ed$$

where e is the electron charge, τ is the carrier lifetime and d is the width of the recombination region (that is, the heterojunction spacing). In a typical GaAs-laser diode, ΔN at lasing threshold is about 2 × 1018 cm⁻³ at room temperature.8 To minimize the threshold current density, we restrict the width of the recombination region by placing the heterojunction that forms the potential barrier for minority carriers closer to the injecting heterojunction than the diffusion length. It is, however, essential that the heterojunction interfaces be relatively defect free in order to prevent excessive nonradiative recombination of the injected carriers.

The nonradiative loss of carriers at an interface is characterized by the recombination velocity S of that interface. Under the usual laser operating conditions we can express the effective recombination rate due to the presence of the interface as

$$\frac{1}{\tau_{\rm eff}} \approx \frac{1}{\tau_0} + \frac{2S}{d}$$

where $1/\tau_0$ is the rate in the absence of an interface. The internal quantum efficiency is given by

$$\eta_{\rm i} \approx \tau_{\rm eff}/\tau_0$$

so that

$$\eta_i \approx (1 + 2S\tau_0/d)^{-1}$$

In typical cw laser diodes d=0.3 microns, and $\tau_0=10^{-9}$ sec. Therefore, for an internal quantum efficiency of 50% (a reasonable lower limit), we would require $S \le 2 \times 10^4$ cm/sec.

The single most important contribution to S is from nonradiative-recombination states introduced at the heterojunction due to the lattice-parameter mismatch between the two materials. If this mismatch is kept below 0.1%, S will be under 2×10^4 cm/sec and cw operation can be anticipated. Experimental data concerning S in GaAs-Al_xGa_{1-x}As heterojunctions indicate that $S \approx 5 \times 10^3$ cm/sec in practical laser structures (where $\Delta a_0/a_0 \lesssim 0.07\%$), a value that is fully satisfactory for narrow-recombination-region devices.

To ensure wave propagation along the plane of the junction, as well as low threshold current density and high efficiency, means must be provided for confinement of stimulated radiation to the region of inverted population (or its close proximity). Two heterojunctions, as indicated in figure 4, provide a controlled degree of radiation confinement due to the higher refractive index in the lowerband-gap recombination region, with the fraction of the radiation confined dependent on the heterojunction spacing d and the refractive-index steps Δn at the lasing wavelength;9 in Al, Ga1-x As-GaAs structures, $\Delta n \approx 0.62 x$ at $\lambda \approx 0.9$ micron. In general it is desirable to equalize the refractive-index steps Δn at all the heterojunctions to prevent the loss of waveguiding that can occur in thin asymmetrical waveguides. However, even with the symmetric double-heterojunction laser. wave confinement within a heterojunction is gradually reduced as its spacing becomes small.

The fraction of the radiation confined to the recombination region of the double-heterojunction laser affects the radiation pattern and threshold current density. The radiation pattern (far-field intensity distribution) is affected because it is determined by the effective source size (near-field intensity distribution); the threshold current density Jth is determined primarily by the optical gain at threshold-only that portion of the optical flux within the recombination region is amplified. Figure 5 shows calculated and experimental values of Jth as functions of d for various values of Δn corresponding to varying heterojunction barrier heights. The lowest Jth value 10 of 475 A/cm^2 is obtained with d = 0.1 micron and $\Delta n = 0.4$ (data corresponding to an Alo.6Gao.4As-GaAs-Alo.6Gao.4As structure). It should be noted that the barrier height also affects the high-temperature performance of lasers.11

The maximum desirable threshold current density for cw operation is below 2000 A/cm², and double-heterojunction laser diodes have routinely operated steadily at room temperature with 0-12% AlAs concentration in the active recombination region. Because of the corresponding band-gap variation this corresponds to an emission wavelength range of 0.9 to 0.8 microns. Room-temperature cw operation of lasers at a wavelength of 1.0 micron has recently been reported for the Ga_xAl_{1-x}As_ySb_{1-y} system, 12 where $J_{\rm th} \approx 2000 \; {\rm A/cm^2}$ was achieved; for the InGaAsP-InP heterojunction system another recent paper reported roomtemperature pulsed operation at low thresholds.12

Stripe geometry

Laser diodes are prepared by cleaving two parallel facets to form the Fabry-Perot cavity. The cw laser diode utilizes a strip geometry to define the lateral dimension, as shown in figure 6. The advantages of this design feature are:

▶ The radiation is emitted from a small region, which simplifies coupling of the radiation into fibers with low numerical aperture.

- The operating current can be minimized because it is relatively simple to form a small active area with photolithographic contacting procedures.
- ▶ The thermal dissipation of the diode is improved because the heat-generating active region is imbedded in an inactive semiconductor medium.
- The small active diode area makes it simpler to obtain a reasonably defect-free area.
- ▶ The active region is isolated from an open surface along its two major dimensions, a factor believed to be important for reliable long-term operation.

In the simplest stripe-contact¹³ structure, the active area is defined by opening a stripe in a deposited SiO₂ film. The surface of the diode is then metallized, with the ohmic contact formed only in the open area of the surface. Other methods that have been used to define the stripe contact include the implantation of deep ionic centers to increase the lateral resistance, and etched moats. Various aspects of the technology were discussed in papers in a special issue on semiconductor lasers of the Journal of Quantum Electronics.¹⁴

Diodes for cw operation are generally designed with the thin p side mounted on copper heat sinks to minimize the thermal resistance of the structure and with a soft solder such as indium to minimize strains in the devices.

The lateral width of the emitting region can be adjusted for a desired operating level by adjusting the stripe width. For example, 100 mW of cw power (from one facet) is obtainable for a stripe width of 100 microns. However, for the typical power levels needed in optical communications (5-10 mW), stripe widths of about 13 microns are used, a dimension that represents a suitable compromise between low operating currents and an appropriate power-emission level. A typical curve of power output as a function of diode current is shown in figure 7. The junction temperature for such devices is only a few degrees above the heat-sink temperature. For example, a temperature differential of 7 K is calculated with a typical power input of 0.5 W at a diode current of 0.3 A, and a thermal resistance of 14 K/W.

The electromagnetic modes of the laser-diode cavity are separable into two independent sets, with transverse-electric and transverse-magnetic polarization. The mode numbers m, s and q define the number of sinusoidal half-wave variations along the three axes of the cavity, transverse, lateral and longitudinal, respectively.

The allowed *longitudinal* modes are determined from the average index of refraction and the dispersion seen by the propagating wave. The Fabry-Perot mode spacing is several angstrom units in typical laser diodes. The *lateral* modes depend on the method used to define the two edges of the diode. In stripe-geometry lasers generally only low-order modes



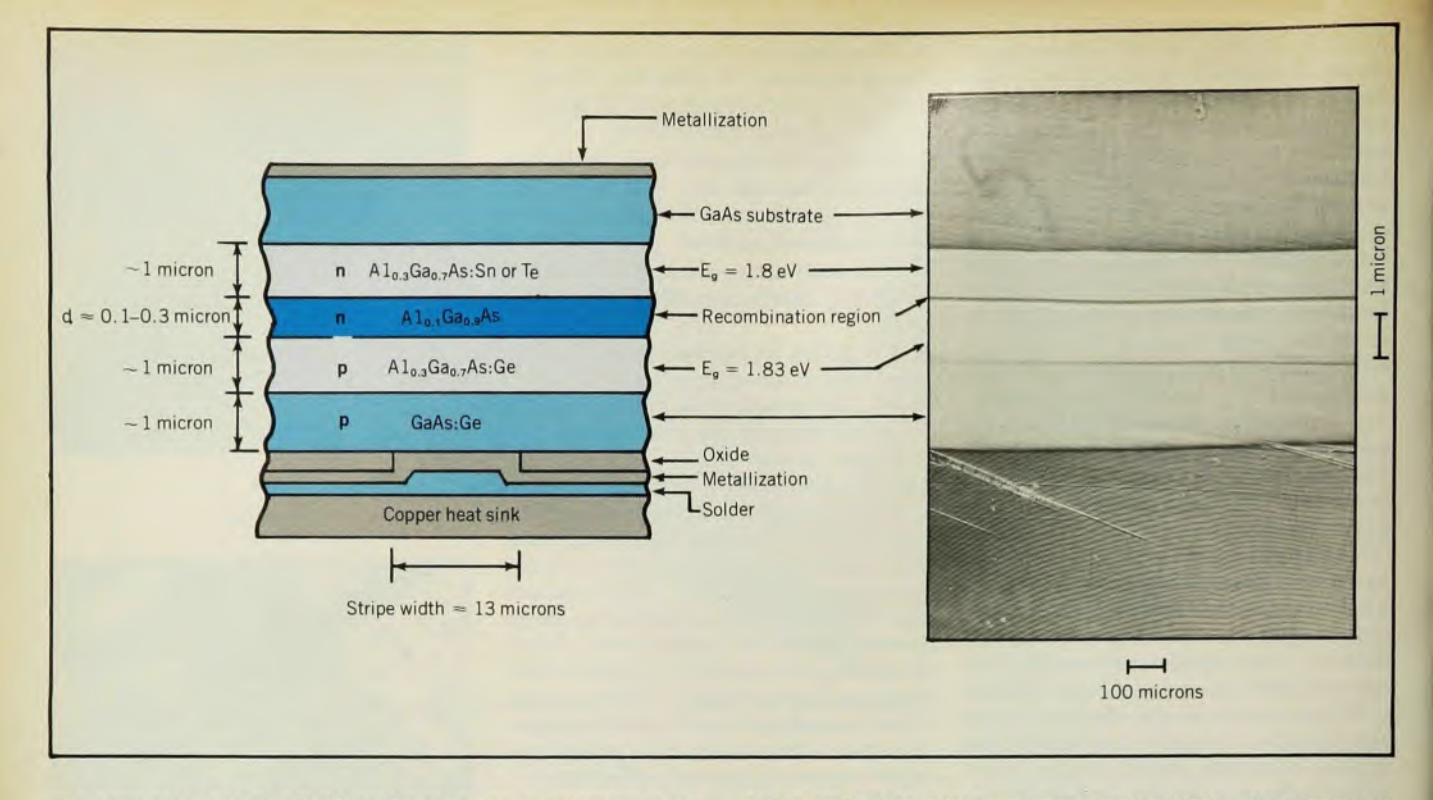
10 microns



Misfit-dislocation arrays in a compositionally graded $\ln_x \text{Ga}_{1-x} \text{P}$ vapor-grown epitaxial layer on a GaP substrate. The top photo is a transmission electron micrograph (ref. 7). Below is shown a cathodoluminescence scan, in which dislocations near the surface appear as non-radiative regions.

are excited; their mode spacings are 0.1-0.2 Å and they appear as satellites to each longitudinal mode. The transverse modes depend on the dielectric variation perpendicular to the junction plane. In the devices discussed here, only the fundamental mode is excited, a condition achieved by restricting the width of the waveguiding region (the heterojunction spacing) to values well under one micron. Therefore, the far-field radiation pattern consists of a single lobe in the direction perpendicular to the junction. (Higherorder transverse modes would give rise to "rabbit-ear" lobes, undesirable for fiber coupling.)

For a laser operating in the fundamental transverse mode, the full angular beam width at half power perpendicular to the junction plane is a function of the near-field radiation distribution. The narrower the emitting region in the direction perpendicular to the junction plane, the larger the beam width. In practical cw laser diodes the beam width is about 30°-50°. The beam width in the plane of the junction (lateral direction) is



The cross section of a typical laser for optical communications is depicted in a schematic illustration (left, not to scale) and in a photomicrograph of a sample that has been polished at a shallow angle to produce

high magnification in the transverse direction (right). The "terracing" effect evident on the lower portion of the micrograph, a growth artifact, causes some interface roughness.

typically 5°-10° and varies only slightly with the diode topology and internal geometry. At least one half of the power emitted from one facet can be coupled

2000 Slope = 4800 A cm⁻² micron⁻¹

Mar = 0.10

0.40

0.00 0.1 0.2 0.3 0.4 0.5

HETEROJUNCTION SPACING (microns)

Threshold current density as a function of the heterojunction spacing for $AI_xGa_{1-x}As$ double-heterojunction lasers. The experimental data points are for aluminum-concentration steps Δx of 0.20 (triangles) and 0.65 (circles). The theoretical curves are for the discontinuities in the refractive index Δn shown, where the relation $\Delta n = 0.62 \Delta x$ has been assumed to apply.

into a multimode step-index fiber with a numerical aperture of 0.14 and a core diameter of 80 microns.

While operation in the fundamental transverse mode is easily achieved, most narrow-stripe laser diodes operate with several longitudinal modes, and therefore emit over a 10–30 Å spectral width, although some units can emit several milliwatts in a single mode. Figure 8 shows the emission spectrum from such a device operating in the fundamental lateral and transverse mode and a single longitudinal mode. The line width is 0.15 Å and the power emitted is 3 mW.

Methods of modulating the laser output vary widely depending upon the application. For fast-pulse modulation, the diode is biased with a current near the threshold current and then pulsed to an appropriate level above threshold. If no bias is applied, there is a lasing delay (related to the spontaneous carrier lifetime) before the carrier population becomes fully inverted and the device turns on. This delay, of several nanoseconds in a typical situation, vanishes if the laser is biased to threshold.

Light-emitting diodes

The spectral bandwidth of the LED is typically $1-2\ kT$ (300–600 Å) at room temperature, hence one to two orders of magnitude broader than that of the typical laser diode. Because of the spectral dispersion in fibers, this may limit the long-distance applications of fiber communications with LED's. Furthermore, the coupling efficiency of LED's into

low-numerical-aperture fibers is much lower than that of laser diodes. However, the LED has the advantage of a simpler construction and a smaller temperature dependence of the emitted power. For example, the spontaneous output from an LED may decrease by a factor of only 1.5–2 as the diode temperature increases from room temperature to 100 deg C (at constant current), while the output of a laser diode would be typically decreased by more than a factor of 3.

The topology of light-emitting diodes is designed to minimize internal reabsorption of the radiation, allow high-current-density operation and maximize the coupling efficiency into fibers. While the structures used are applicable to all materials, most of the work on devices suitable for communications reported so far has been on $Al_x Ga_{1-x} As$.

Two basic diode configurations for optical communications have been reported: surface emitters15 and edge emitters. 16,17 In the surface emitter, the recombination region is placed close to a heat sink, as shown in figure 9. A well is etched through the GaAs substrate to accommodate a fiber. The emission from such a diode is essentially isotropic. The edge-emitting heterojunction structures, similar to the laser geometry of figure 6, uses the partial internal waveguiding of the spontaneous radiation due to the heterojunctions to obtain improved directionality of the emitted power in the direction perpendicular to the junction plane. The lateral width of the emitting region is adjusted for the fiber dimension,

Announcing the 3400

Interactive Graphics Display...



Welcome to 1980.

Introducing a totally new graphics display system with years-ahead performance at years-ago prices: the Vector General 3400.

Featuring a new standard of hardware modularity and firmwear flexibility, the 3400 has a system organization designed to keep pace with advances in minicomputer hardware and operating systems technology.

The 3400 hardware features 3D Digital Transformations, a 1,600-to-1 Dynamic Range, Clip/Zoom/Window, Perspective, unique user aids (Hit/Select/Pick/Edit), and an internal refresh buffer that yields a dramatic reduction in host computer loading.

Complementing the 3400's advanced hardware and firmwear, there is a powerful new software system featuring VGAM (Vector Graphics Access Method) a macro-oriented handler with facilities for efficient graphics resources management.

The technology of the 3400 will be commonplace in the 1980's; with Vector General's 3400, you can have it today.

VECTOR GENERAL

Vector General: Years Ahead.

21300 Oxnard Street • Woodland Hills, California 91364 • Phone (213) 346-3410 • TWX 910-494-2764





M-40R LIGHT MODULATOR



D-70R LASER DEFLECTOR

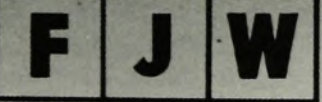


RAMP FREQUENCY GENERATOR



D-150R LASER DEFLECTOR

Acousto-Optics Division by FJW Industries. As a leader in the field of Electro-optical Systems and infrared viewing devices, we at FJW await the opportunity to serve your Acousto-Optics needs.



the acquisition of the Zenith

INDUSTRIES

215 East Prospect Avenue Mount Prospect, III. 60056 Phone 312/259-8100

> Booth =35, CLEOS Circle No. 27 on Reader Service Card



GERMANIUM RESISTANCE THERMOMETER

"The Courier Of The Low Temperature Scales"

ACCURATE - SENSITIVE - RELIABLE OVER 10 YEARS OF SERVICE

CryoCal Calibration Service 1.5 to 100K 57 Data Points

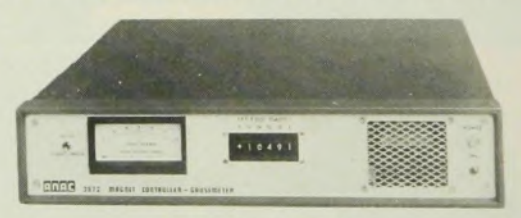
Computer Interpolation Tables

for details write or phone

P. O. Box 10176 1371 Avenue "E" Riviera Beach, Fla. 33404, U.S.A. Call 305 842-4750

Circle No. 28 on Reader Service Card

MAGNET CONTROLLER/GAUSSMETER



ANAC Model 3672

- Direct magnet field control using any programmable Power Supply.
- Hall effect field sensing probes.
- 5 digit field setting (±1 gauss accuracy).
- BCD digital remote programming.
- -30 to +30 kgauss control range.
- -30 to +30 gauss incremental field measurement range.
- Analog recorder outputs.
- Versatile gain and phase compensation controls.

Call or write for complete technical specifications -



ANAC Inc. P.O. Box 7453, Menlo Park, CA 94025 Tel (415) 322-8664

AD-11-PT

Circle No. 29 on Reader Service Card

but is typically 50-100 microns.

Surface-emitting and edge-emitting structures provide several milliwatts of power output in the 0.8-0.9 micron spectral range operated at drive currents of 100-200 mA (2000-4000 A/cm²). The coupling loss into step-index fibers with a numerical aperture of 0.14 is about 17-20 dB for surface emitters and 12-16 dB for edge-emitting diodes, compared to about 3 dB for an injection laser. Since the coupling loss decreases as the inverse square of the numerical aperture, much more power can, of course, be coupled into larger-numerical-aperture fibers. But with these coupling losses, Alo.1Gao.9As double-heterojunction LED's can provide about 0.1 mW into a 0.14 NA, 80 micron diameter fiber at drive currents of about 200 mA with an applied voltage of 1.7 V.

Let us turn now to the modulation problem. The relation between the optical power output of an LED (with constant peak current) and the modulation frequency is given by

$$\frac{P(\omega)}{P_0} = \frac{1}{[1 + (\omega \tau)^2]^{1/2}}$$

where τ is the lifetime of the injected carriers in the recombination region and P_0 is the dc power emission. (However, parasitic circuit elements can reduce the modulated power range below this value.)

It is evident that a high-speed diode requires the lowest possible value of τ , but without sacrifice in the internal quantum efficiency. Low values of τ are obtained at high doping levels; but in GaAs and related compounds, a high density of nonradiative centers is formed when the dopant concentration approaches the solubility limit at the growth temperature. Of the devices reported so far, germanium-doped double heterojunction LED's have exhibited modulation capability (at

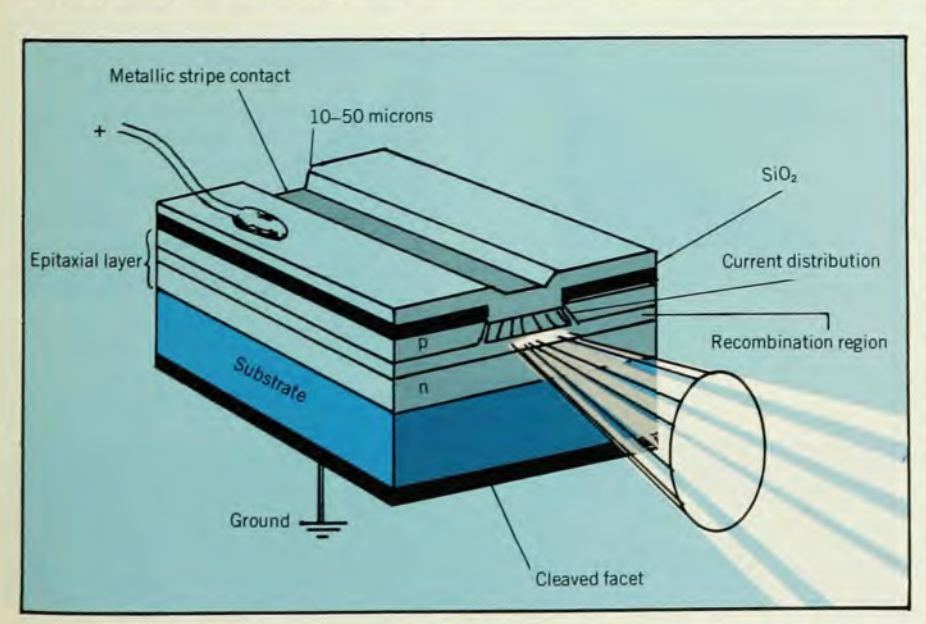
the 3-dB point) to about 200 MHz.¹⁶ The use of germanium is advantageous because it can be incorporated into GaAs to concentrations of about 2 × 10¹⁹ cm⁻³, thus providing lifetimes on the order of one nanosecond without unduly reducing the internal quantum efficiency.

With regard to LED's for 1.0-1.1 micron emission, surface-emission outputs of about 1 mW have been achieved with InGaAs structures¹⁸ and further progress is expected, particularly with lattice-matched InGaAs-InGaP heterojunction structures.¹⁹

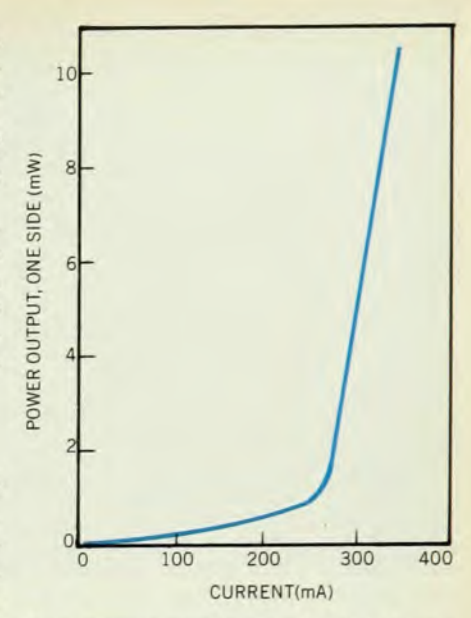
Device reliability

In any practical optical communications system, component reliability is of great concern. It has been a major research goal to identify and correct the myriad of failure mechanisms that plagued early electroluminescent devices.20 The failure modes have since been identified as either facet- or bulkrelated; they can be of a gradual or a catastrophic nature. Facet degradation is specifically a laser problem because the facets are the mirrors that define the Fabry-Perot resonator. Bulk degradation, on the other hand, can occur in both LED's and lasers. Most failure mechanisms have been eliminated as the overall technology (crystal growth, device fabrication) has matured, but active concern still exists for those remaining few that may limit ultimate operating life. Insufficient data exist for mean time to failure, which, for telephone applications, is in the 100 000-hr range. A comprehensive model for laser-facet failure does not exist but considerable phenomenological data have been accumulated.

Facet failure due to intense light fields is a well known phenomenon in solid-state lasers, and has been found to occur in



Schematic of a typical cw heterojunction laser, drawn upside down relative to figure 4 to show the stripe contact. Diffraction causes the vertical spreading of the beam.



Optical power output from one facet of a typical aluminum gallium arsenide cw laser as a function of the drive current, measured at room temperature. Figure 7

semiconductor lasers of all types under varying conditions when the optical power density in the recombination region reaches the order of 10⁶ W/cm². The appearance of the damaged laser facets suggests local dissociation of the material as well as "cracking" in some cases.

The critical damage level is also a function of the pulse length t, decreasing as $t^{-1/2}$, over the range of 20 to 2000 nsec. It is not surprising, therefore, that facet damage can occur in room-temperature laser diodes operating cw at their maximum emission levels (even with relatively low total power). Because of the nonuniform radiation distribution in the plane of the junction in stripe-contact lasers, it is difficult to establish damagelevel criteria in terms of the total power output. However, the damage threshold for 100 nsec pulses is about ten times higher than for cw operation of diodes selected from the same group.21

In addition to the dependence on optical flux density and pulse length, it has been found that ambient conditions. specifically moisture and surface flaws (scratches, dirt particles), can lead to premature facet failure. To remove these limitations, lasers must be operated at a specific maximum power level and the facets must be passivated with protective dielectric coatings for isolation from their surroundings. For cw lasers the operating range of linear power density is about 1 mW per micron of stripe width. Facet failure, at least in its early stages, commonly manifests itself as a decrease in differential quantum efficiency without an increase in threshold current density.

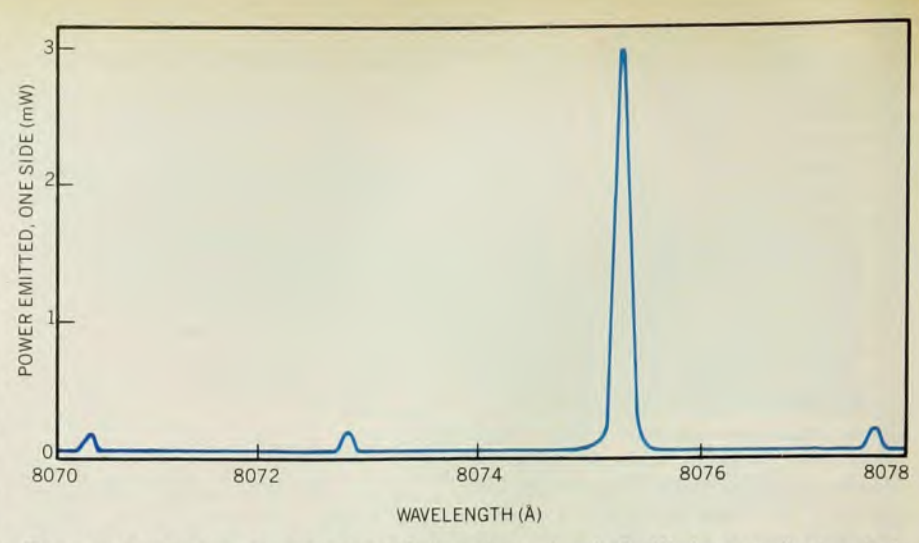
Bulk degradation, the other failure mode, is accompanied by an increase in threshold current density and a decrease in differential quantum efficiency due to a reduction in *internal* quantum efficiency and an increase in the absorption coefficient. The reduction in output power may be small but need not be—if the device is a laser operated near threshold it may turn off completely. In either case a small adjustment in current will restore the output to its initial value. With such a feedback system, a definition of operating life becomes somewhat arbitrary and system-dependent.

The available evidence suggests that the gradual degradation process results from an increase in the concentration of nonradiative centers in the recombination region. These defects are initiated by the growth of flaws initially present in the recombination region of the diode. Point defects may also diffuse into the active region from adjacent flawed regions. Detrimental flaws include dislocations and impurity precipitates. One prominent effect in some degraded lasers is the formation of "dark lines" in regions where the luminescence is gradually extinguished.22 These regions have been identified as large dislocation networks that, having started as smaller pre-existing dislocation networks, grow by the immigration of vacancies or interstitials.23 In addition, more dispersed nonradiative centers such as native point defects apparently contribute to the degradation process.

It has been suggested that a multiphonon emission process resulting from nonradiative electron-hole recombination gives rise to an intense vibration of the center, which reduces its displacement energy.²⁴ (Whether any point defects are actually *formed* within the recombination region remains unclear.) Hence, if nonradiative electron-hole recombination occurs, say at the damaged surface of a diode (as in the case of the sawed-edge diode experiment described in reference 25), it accelerates the motion of point defects into the active region of the device.

The stoichiometry of the material in the active region or in close proximity to it is believed to affect the reliability of the device, as does the nature of the dopant. A modification of initial stoichiometry may account for the improved degradation resistance of diodes fabricated with Al_{0.1}Ga_{0.9}As rather than GaAs in the recombination region. Finally, regions where nonradiative recombination occurs will tend to grow in size, leading to the strongly nonuniform degradation process that is commonly observed.

Enormous progress has been made since 1970 in eliminating many degradation mechanisms in lasers and LED's by careful attention to the liquid-phase epitaxial growth and device processing. Facet passivation with dielectric coatings has virtually eliminated facet damage as an important failure mode in cw lasers. The ultimate operating lifetime of state-of-the-art devices remains undetermined,



The spectral output from one facet of an AlGaAs cw laser. It emits 3 mW when operating in a single longitudinal mode and in the fundamental transverse and lateral mode.

Figure 8

but accumulated data exists on devices in operation at constant current for times well in excess of 14 000 hr without a serious drop in output power. Two examples of lifetime data taken over many hours of operation on our more recently fabricated diodes are:

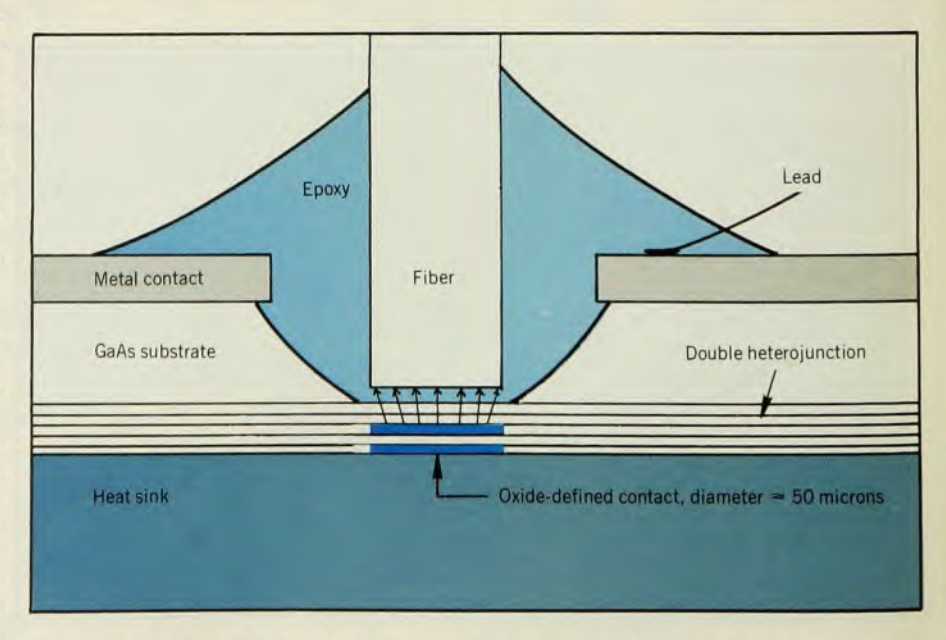
- ▶ In a lot of AlGaAs LED's emitting about 1 mW at 0.8 microns, the emitted power remained constant within 5% in 14 000 hours of operation;
- ▶ In AlGaAs cw lasers emitting between 5 and 10 mW from one facet at a wavelength of 0.82 microns, the maximum deviation was less than 20% in 10 000 hours.

Laser diodes with unpassivated facets have operated for more than 15 000 hours but with more significant reduction in power output at fixed current. These data contrast sharply with those of a few years back, when the best operating life

was a few hundred hours under similar conditions.

Future devices

With regard to future work, heterojunction structures of AlGaAs emitting in the 0.80-0.85 micron spectral range have progressed to the point where practical systems applications of lasers and LED's are becoming possible. This has been the result of extensive research on the properties of materials and methods of synthesis as well as the identification of major factors affecting the operating lifetime of these devices. Research is now under way on devices emitting in the 1.0-1.1 micron range, which offers some potential advantages in reduced fiber absorption and dispersion. These devices involve more complex material problems than the Al-GaAs devices because of the need to use dissimilar alloys to match the lattices.



An etched-well surface-emitting LED designed for fiber optics, in a schematic cross section. The emission from this type of diode is essentially isotropic. (Reference 15) Figure 9

References

- 1. H. Kressel, H. Nelson, RCA Review 30, 106
- 2. I. Hayashi, M. B. Panish, P. W. Foy, IEEE J. Quantum Electron. 5, 211 (1969).
- 3. Zh. I. Alferov, V. M. Andreev, E. L. Portnoi, M. K. Trukan, Sov. Phys. Semiconductors 3, 1107 (1970).
- 4. I. Hayashi, M. B. Panish, P. W. Foy, S. Sumski, Appl. Phys. Letters 17, 109 (1970).
- 5. H. Kressel, F. Z. Hawrylo, Appl. Phys. Lett. 17, 169 (1970).
- 6. C. B. Duke, N. Holonyak Jr, PHYSICS TODAY, December 1973, page 23.
- 7. G. H. Olsen, J. Crystal Growth 31, 223
- 8. F. Stern, IEEE J. Quantum Electron. 9, 290 (1973); A. Yariv, Quantum Electronics, 2nd edition, Wiley, New York (1975); J. I. Pankove, Optical Processes in Semiconductors, Prentice-Hall, Englewood Cliffs (1971); S. E. Miller, Tingye Li, E. A. J. Marcatili, Proc. IEEE 61, 1726 (1973).
- 9. J. K. Butler, H. Kressel, I. Ladany, IEEE J. Quantum Electron. 11, 402 (1975); W. P. Dumke, ibid, page 400; P. R. Selway, A. R. Goodwin, J. Phys. D 5, 9041 (1972); H. C. Casey Jr, M. B. Panish, J. L. Merz, J. Appl. Phys. 44, 5470 (1973).
- 10. M. Ettenberg, Appl. Phys. Lett. 27, 652
- 11. A. R. Goodwin, J. R. Peters, M. Pion, G. H. B. Thompson, J. E. A. Whiteway, J. Appl. Phys. 46, 3126 (1975).
- 12. R. E. Nahory, M. A. Pollak, E. D. Beeke, J. C. DeWinter, R. W. Dixon, Appl. Phys. Lett. 28, 19 (1976); J. J. Hsieh, Appl. Phys. Lett. 28, 283 (1976).
- 13. J. C. Dyment, Appl. Phys. Lett. 10, 84 (1966).
- 14. IEEE J. Quantum Electron. 11, 381-562 (July 1975).
- 15. C. A. Burrus, B. I. Miller, Opt. Commun. 41, 307 (1971).
- 16. M. Ettenberg, H. F. Lockwood, J. Wittke, H. Kressel, Technical Digest of the 1973 International Electron Devices Meeting, Washington, D.C., page 317.
- 17. H. Kressel, M. Ettenberg, Proc. IEEE 63, 1360 (1975).
- 18. C. J. Nuese, R. E. Enstrom, IEEE Trans. Electron. Devices 19, 1067 (1972).
- 19. C. J. Nuese, G. H. Olsen, Appl. Phys. Lett. 26, 528 (1975).
- 20. H. Kressel, H. F. Lockwood, J. de Physique C 3, Suppl. 35, 223 (1974).
- 21. H. Kressel, I. Ladany, RCA Review 36, 230 (1975).
- 22. B. C. DeLoach, B. W. Hakki, R. L. Hartman, L. A. D'Asaro, Proc. IEEE 61, 1042 (1973); R. Itoh, H. Nakashima, S. Kishino, O. Nakada, IEEE J. Quantum Electron. 11, 551 (1975).
- 23. P. Petroff, R. L. Hartman, Appl. Phys. Lett. 23, 469 (1973).
- 24. R. D. Gold, L. R. Weisberg, Solid-State Electron. 7, 811 (1964).
- 25. I. Ladany, H. Kressel, Appl. Phys. Lett. 25, 708 (1974).
- 26. M. Ettenberg, H. Kressel, Appl. Phys. Lett. 26, 478 (1975); P. G. McMullin, J. Blum, K. K. Shih, A. W. Smith, G. R. Woolhouse, Appl. Phys. Lett. 24, 595 (1974).

SURFACE SCIENCE THIN FILMS ULTRA HIGH VACUA

23rd National Symposium of the American Vacuum Society Sept. 21-23, 1976 Palmer House Chicago

MEETING

Abstracts Deadline 5/24/76

Invited papers; partial

Photovoltaic Heterojunctions D. L. Feucht

Heterojunctions in Integrated Optics

..... D. R. Scifres

Interactions in Absorbed Layers

Synchrotron Photoemission Studies of Clean and Chemisorbed Surfaces

.....G. J. Lapeyre

Fusion Reactor Wall ProblemsL.Pittenger

Vacuum Metallurgy and Critical Resources

. F. Wood Pumping and Vacuum Require-

ments for Fusion Devices

Fusion Device Materials Research

Blistering and Wall Erosion

in Fusion ReactorsT. Rossing

Light Ion Behavior in Solids

. O. S. Oen

Structural Defects in Dielectric Films

Program Chairman:

John L. Vossen **RCA** Laboratories Princeton, NJ 08540 (609) 452-2700

Inficon

Kearns Group

Kimball Physics

Lammert Industries

Leybold-Heyaeus

R.D. Mathis

Electronics

Plasma Therm

Scientific

Sargent-Welch

Sloan Insts

Sylvania

Technics

Torr Vacuum

Ulvac N Am

Vacuum Insts

Vacuum Res

Uthe Tech

Vacoa

Varian

Veeco

Ultek/PE

3M

Polycold Systems

MKS Insts

Physical

Precision

(Exhibitors 4/1/76)

Aero Vac

Airco-Temescal

Air Products

& Chemical

Alcatel

Calflex

CENCO

Ceramaseal CHA Industries

Circuits

Processing Commonwealth

Scientific

Cooke Vacuum

Corning Glass

Crawford Fitting

CTI

Datametrics

Edwards High Vac

EM Labs

E.T. Equipment

Extranuclear

Ferrofluidics

GCA/McPherson

Granville-Phillips

Hastings-Raydist

High Vac App

Show Information:

Ed Greeley, A.I.P. 335 E. 45th Street N.Y., N.Y. 10017 (212) 685-1940